APPLYING TAFKAA FOR ATMOSPHERIC CORRECTION OF AVIRIS OVER CORAL ECOSYSTEMS IN THE HAWAI'IAN ISLANDS

James A. Goodman,[1] Marcos J. Montes,[2] and Susan L. Ustin[1]

1. INTRODUCTION

Growing concern over the health of coastal ecosystems, particularly coral reefs, has produced increased interest in remote sensing as a tool for the management and monitoring of these valuable natural resources. Hyperspectral capabilities show promising results in this regard, but as yet remain somewhat hindered by the technical and physical issues concerning the intervening water layer. One such issue is the ability to atmospherically correct images over shallow aquatic areas, where complications arise due to varying effects from specular reflection, wind blown surface waves, and reflectance from the benthic substrate. Tafkaa, an atmospheric correction algorithm under development at the U.S. Naval Research Laboratory, addresses these variables and provides a viable approach to the atmospheric correction issue. Using imagery from the Advanced Visible InfraRed Imaging Spectrometer (AVIRIS) over two shallow coral ecosystems in the Hawai'ian Islands, French Frigate Shoals and Kane'ohe Bay, we first demonstrate how land-based atmospheric corrections can be limited in such an environment. We then discuss the input requirements and underlying algorithm concepts of Tafkaa and conclude with examples illustrating the improved performance of Tafkaa using the same AVIRIS images.

2. STUDY AREAS

Three AVIRIS flightlines from the 2000 Hawai'ian Islands acquisition were used in this analysis. All three were acquired from the high-altitude ER-2 platform at an altitude of 20 km, thereby producing a nominal pixel size of approximately 17 m. Two of the flightlines cover the southern portion of French Frigate Shoals (Fig. 1), which is a sizeable semi-circular atoll in the remote Northwestern Hawai'ian Islands extending nearly 34 km in width. The area contains a few small exposed sandy islets, but consists mostly of submerged coral reefs and other associated habitats. The two flightlines for this area, f000418t01p03_r01 and f000418t01p03_r02, are significant because they contain overlapping spatial coverage and exhibit substantial differences in specular reflection from the water surface. This overlapping region provides a valuable avenue for evaluating algorithm performance for the same area but under different illumination conditions. The third flightline, f000412t01p03_r08, covers Kane'ohe Bay on the northeast shore of O'ahu. Kane'ohe Bay is a partially enclosed embayment, extending approximately 4 km in width and 13 km in length along a northwest-to-southeast axis. The bay contains fringing reefs, sizeable patch reefs and an extensive protecting barrier reef. Habitat and water quality conditions vary within the bay and the reefs range from coral-dominated to algae-dominant systems. Differences in specular reflection are not as visually apparent in this flightline and thus serve to test algorithm performance under more consistent illumination conditions.

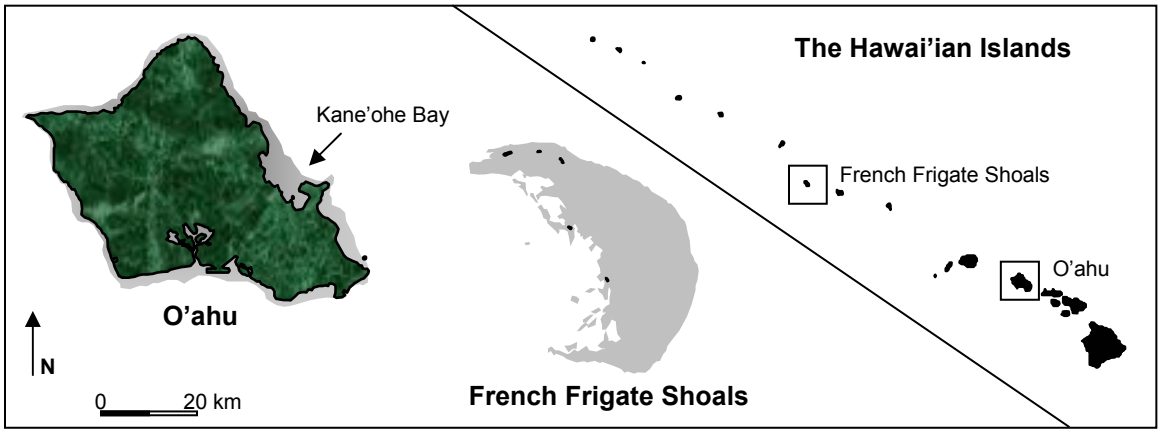

Figure 1. Study areas in the Hawai'ian Islands.

[1] Center for Spatial Technologies and Remote Sensing (CSTARS), Department of Land, Air and Water Resources, University of California, Davis (corresponding author: jagoodman@ucdavis.edu).
[2] Remote Sensing Division, Code 7232, Naval Research Laboratory, Washington, DC.

3. EXAMPLE CORRECTION LIMITATIONS

The Atmospheric CORrection Now (ACORN) software package was selected to provide an example of the potential difficulties of using a land-based atmospheric correction algorithm over water. ACORN (Analytical Imaging and Geophysics, LLC) is a readily available commercial atmospheric correction package that is commonly used in terrestrial hyperspectral applications. Its use here is not intended to identify weaknesses in ACORN nor be critical of its use on other datasets, but merely to illustrate a situation where limitations in terrestrial algorithms become evident when applied to an aquatic system.

3.1 ACORN Methods

ACORN requires radiometrically calibrated radiance data as input and produces estimates of apparent reflectance based on MODTRAN radiative transfer calculations (AIG, 2001). Other inputs to the model include: a description of sensor characteristics for the wavelength position, full-width half-max, gain, and offset for each band; the average elevations of the sensor and the image; and scene specific information identifying the latitude, longitude, time and date of the image center. For application to the three AVIRIS flightlines considered here, the algorithm was run in Mode 1 (hyperspectral atmospheric correction of complete image) with a tropical atmospheric model, using the 940 and 1140 nm bands to derive water vapor, and allowing the model to estimate atmospheric visibility based on image characteristics. Options were also selected to reduce the effects of spectral mismatch and minimize the errors associated with the 1400 and 1900 nm water vapor bands and other smaller spectral artifacts.

3.2 ACORN Results

Reflectance outputs for two locations in French Frigate Shoals are illustrated in Fig. 2. The first area (2A) depicts results for a shallow location with significant reflectance from the benthic surface and the other area (2B) for a deep-water location with no influence from the bottom. The two lines in each graph illustrate output for the same geographic location as derived from the two separate overlapping images, thereby providing a direct comparison of model performance for the same area but under differing amounts of specular reflection. Keeping in mind that reflectance in longer wavelengths should approach zero due to the absorption properties of water, it is apparent in all situations that the resulting reflectance exhibits a shift to higher values. Other observations reveal that this shift is not spatially uniform throughout the image nor is it dependent on water depth. Furthermore, it is uncertain whether this shift is constant across all wavelengths for a given pixel or whether it is independent of wavelength. There is also an inconsistency in results between the two overlapping images, which is presumably a function of the significant differences in specular reflection. Results for two locations in Kane'ohe Bay, an image with far less visually apparent variation in specular reflection, are presented in Fig. 3. A similar shift in reflectance is again apparent. The presence of this shift along with the observed inconsistencies illustrates a limit in the quantitative application of land-based atmospheric correction algorithms over water.

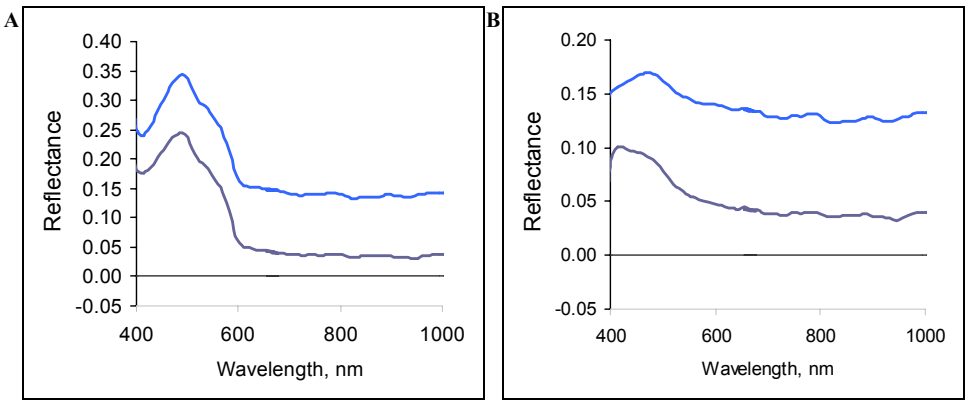

Figure 2. ACORN derived reflectance for French Frigate Shoals from two overlapping flightlines: (A) shallow area with strong bottom influence; and (B) deep water.

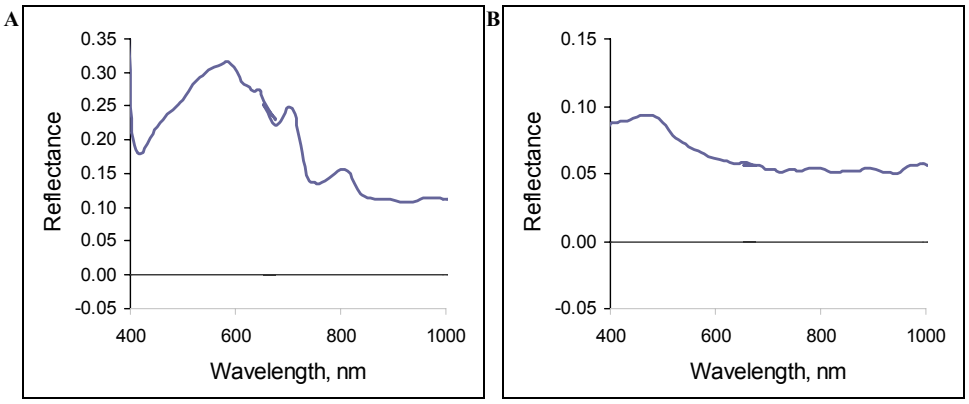

Figure 3. ACORN derived reflectance for Kane'ohe Bay: (A) shallow area with strong bottom influence; and (B) deep water.

4. TAFKAA

Tafkaa is an extensively modified version of the ATmospheric REMoval algorithm (ATREM; Gao and Davis, 1997; Gao et al., 1993) that has been specifically adapted to address the confounding variables associated with aquatic remote sensing applications (Gao et al., 2000; Montes et al., 2001, 2003a, 2003b). It uses information supplied in the input files and by the spectral characteristics of the input radiance data to generate atmospheric correction parameters from a series of lookup tables. Given input of radiometrically corrected at-sensor radiance data, Tafkaa provides output in the form of reflectance ($\rho = \pi L_w/E_d$), remote sensing reflectance (L_w/E_d), normalized water-leaving radiance ($[L_w]_N$), or observed reflectance (ρ_{obs}). Tafkaa also has an associated procedure called Mask that allows for masking of land and clouds. Presented below is an introduction to the Mask and Tafkaa algorithms, an overview of their input requirements, and a discussion of results as applied to the AVIRIS images of French Frigate Shoals and Kane'ohe Bay.

4.1 Mask

The Mask algorithm (undergoing development) provides a utility for identifying and masking land, cirrus clouds, and low altitude clouds. Tafkaa requires knowledge of which pixels are not aquatic because the underlying assumptions used for determining the appropriate aerosol model and optical depth over water do not apply to land or clouds. Thus, identification of land pixels allows Tafkaa to properly process land pixels using a different procedure. Additionally, independent identification of cirrus clouds may allow for correction of some of these pixels at a later date (Gao et al., 1998). Criteria for creating each of the three masks are based on values of observed reflectance, ρ_{obs}, as calculated from the input radiance data and approximations of extra-terrestrial solar irradiance. The land mask employs a user-defined threshold on either a single wavelength (also configurable) or on a normalized difference index, NDI. The cloud masks are both determined by user-defined thresholds on particular wavelengths, 1375 nm for cirrus clouds and 940 nm for low altitude clouds. A complete description of all configurable parameters can be found in the *Mask User's Guide*. Output is in BSQ image format, where bands in the image represent each of the resulting masks (0 is not masked and 100 is masked). The land mask selected for this analysis was the NDI option, $(\rho_{obs}(860nm)-\rho_{obs}(660nm))/(\rho_{obs}(860nm)+\rho_{obs}(660nm))$, with land assigned to pixels where NDI > 0.05. The cirrus cloud mask was identified by pixels where $\rho_{obs}(1375nm) > 0.0025$ and the low altitude cloud mask by pixels where $\rho_{obs}(940nm) > 0.1$. Example Mask output is presented in Fig. 4 for an area of Kane'ohe Bay centered on Moku O Lo'e (Coconut Island). Results reveal good agreement for the land areas of the land mask, but also appear to include areas of cloud as land. The cirrus and low altitude cloud masks show even less robust performance with these particular settings. Nevertheless, when used together the overall mask output does an acceptable job of leaving the aquatic areas unmasked while sufficiently masking land and clouds.

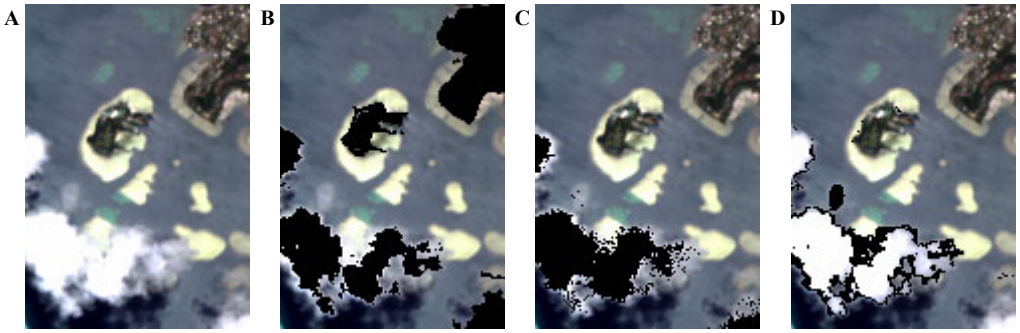

Figure 4. Mask output for Kane'ohe Bay with Moku O Lo'e (Coconut Island) shown at center: (A) unmasked RGB; (B) land mask; (C) cirrus cloud mask; and (D) low altitude cloud mask.

4.2 Atmospheric Correction

The underlying equation for Tafkaa considers total at-sensor radiance to be a function of path radiance, specular reflection from the water surface and reflected radiance from the water, which is a composite function of reflected radiance from the water column and bottom passing through the air-water interface. The algorithm interpolates correction parameters from lookup tables generated using a vector radiative transfer program and ultimately provides a pixel-by-pixel solution for the radiance reflected from the water. Input parameters include the sensor altitude, average ground elevation, wind speed, and level of atmospheric ozone (estimated using data from the TOMS sensor). A full description of these and other input parameters can be found in the frequently updated *Tafkaa User's Guide*. Tafkaa was run on the three AVIRIS flightlines with a tropical atmospheric model, all available gaseous absorption calculations (H_2O, CO_2, O_3, N_2O, CO, CH_4, O_2) and by excluding use of urban aerosols from the offered aerosol solutions. The model also allows the user to select bands from a set of options to signify wavelengths with no apparent water leaving radiance for determining aerosol computations (Fig. 5). Bands selected for French Frigate Shoals and Kane'ohe Bay included the 1040, 1240, 1640 and 2250 nm wavelengths. The most recent version of Tafkaa additionally includes a feature allowing for computations to explicitly account for pixel-by-pixel variations in view and illumination geometry (Montes et al., 2003a). Using this option proved to significantly enhance Tafkaa's ability to account for cross-track variations in specular reflection for the flightlines considered here. The additional input parameters for this option were the date, time and location of the center for every image line, as well as the AVIRIS cross-track pointing geometry.

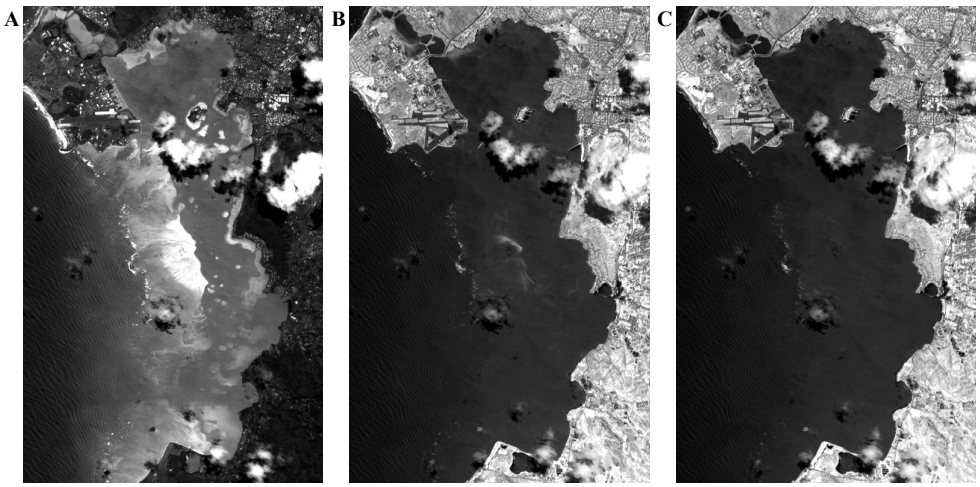

Figure 5. Observed radiance for three bands of radiometrically corrected AVIRIS data for Kane'ohe Bay: (A) 550 nm; (B) 860 nm; and (C) 1040 nm. Note that bottom is strongly visible at 550 nm, only slightly apparent at 860 nm, and no longer evident at 1040 nm.

4.3 Tafkaa Results

Reflectance results produced from Tafkaa are presented for the same areas as examined above and output is again presented in the form of reflectance. Fig. 6 illustrates results for French Frigate Shoals and Fig. 7 for Kane'ohe Bay. Unlike results from the land-based algorithm, reflectance values in the Tafkaa output appropriately tend towards zero at longer wavelengths, which holds true throughout each of the images. A certain amount of spectral mismatch is evident in the results (e.g., around the 940 nm water vapor absorption feature), but overall the generated values are reasonable. Although it is possible to analyze and even ameliorate the spectral mismatch (Gao et al., 2003), this ability has not yet been built into Tafkaa. Results for the same geographic areas from the two different flightlines in French Frigate Shoals (Fig. 6) are substantially more similar than those produced using the land-based algorithm (Fig. 2). Although this comparison is not perfect, the level of agreement between the two flightlines is encouraging considering the sizeable differences in specular reflection. Thus, analysis of spatial and temporal changes within and between flightlines can be performed with greater confidence that differences are a function of changing water and bottom conditions and not artifacts of the atmospheric correction routine. Overall, it is evident that there is still room for improvement, but improved results demonstrate that Tafkaa more successfully generates acceptable reflectance output for atmospheric correction over water and produces improved results over land-based algorithms.

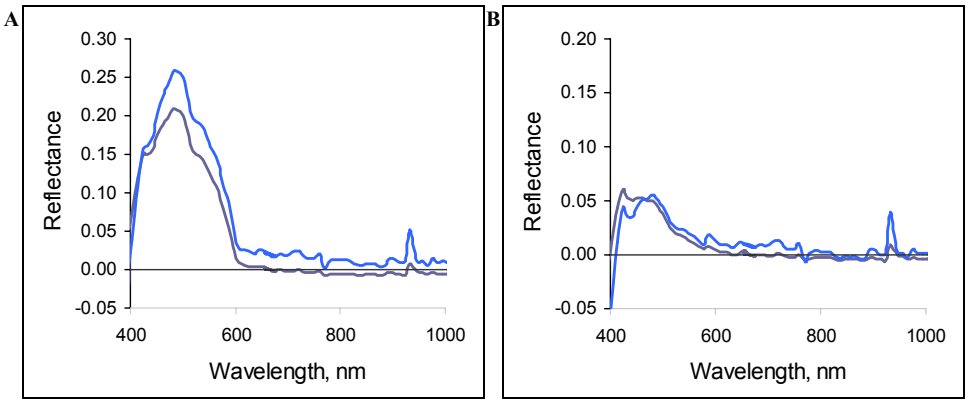

Figure 6. Tafkaa derived reflectance for French Frigate Shoals from two overlapping flightlines: (A) shallow area with strong bottom influence; and (B) deep water.

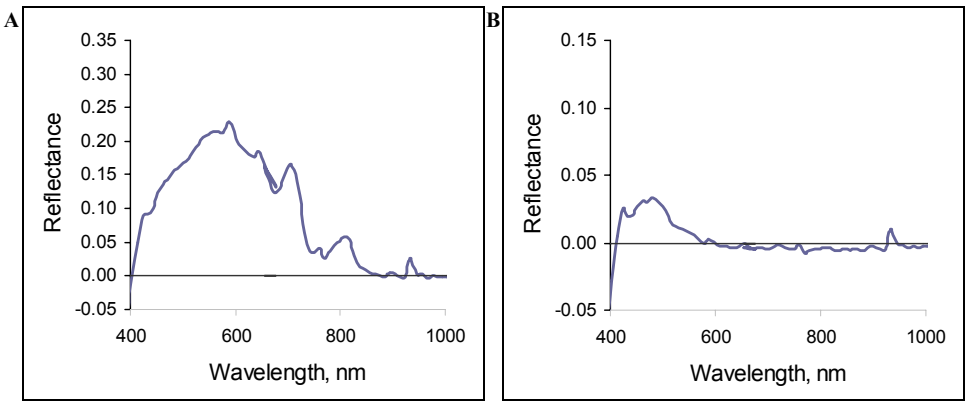

Figure 7. Tafkaa derived reflectance for Kane'ohe Bay: (A) shallow area with strong bottom influence; and (B) deep water.

5. CONCLUSION

Analysis of benthic habitats in shallow aquatic areas is complicated by the confounding effects of the overlying water column and the air-water interface. This means that in addition to atmospheric influences, at-sensor measurements over water are also a function of water properties, surface waves, water depth, bottom characteristics and illumination conditions. This presents a more challenging environment than typical atmospheric correction problems over land, and thus is not necessarily suitable for land-based correction algorithms. For instance, as shown in the examples above, there are situations where results from land-based algorithms can be inconsistent and of limited utility. In contrast, Tafkaa is designed to directly address the aquatic correction issues. The Tafkaa results illustrated above demonstrate physically realistic reflectance output and uniformity within and between images. This represents not only an improved atmospheric correction, but also a more appropriate foundation from which to next address issues of water column correction and spectral analysis of the benthic surface. Thus, improvements in the atmospheric correction will ultimately lead to advances in the evaluation of benthic habitats.

6. ACKOWLEDGEMENTS

This work was supported by NASA Headquarters under the Earth System Science Fellowship Grant NGT5-ESS/01-0000-0208. It is has been made possible by the Department of Land, Air and Water Resources and the Center for Spatial Technologies and Remote Sensing at the University of California, Davis. Additional support was also provided by the University of California Pacific Rim Research Program, the California Space Institute Graduate Student Fellowship Program, the Canon National Park Science Scholars Program and NASA's Jet Propulsion Laboratory. Furthermore, the authors would like to thank the Hawaiian Institute of Marine Biology for their assistance and Paul Sjordal for his untiring efforts in the field. Author MJM acknowledges support from the U.S. Office of Naval Research.

7. REFERENCES

Analytical Imaging and Geophysics, LLC (AIG), 2001, "ACORN User's Guide," Boulder, Colorado.

Gao, B.-C., K.H. Heidebrecht and A.F.H. Goetz, 1993, "Derivation of Scaled Surface Reflectance from AVIRIS Data," Remote Sens. Environ., vol. 44, pp. 165-178.

Gao, B.-C. and C.O. Davis, 1997, "Development of a Line-by-Line Based Atmospheric Removal Algorithm for Airborne and Spaceborne Imaging Spectrometers," in Imaging Spectrometry III (M.R. Descour and S.S. Shen, eds.), Proceedings of the SPIE Vol. 3118, pp. 132-141.

Gao, B.-C., Y.J. Kaufman, W. Han and W.J. Wiscombe, 1998, "Correction of Thin Cirrus Path Radiances in the 0.4-1.0 μm Spectral Region Using the Sensitive 1.375 μm Cirrus Detecting Channel," J. Geophys. Res., vol. 103, no. D24, pp. 32169-32176.

Gao, B.-C., M.J. Montes, Z. Ahmad and C.O. Davis, 2000, "Atmospheric Correction Algorithm for Hyperspectral Remote Sensing of Ocean Color from Space," Appl. Optics, vol. 39, no. 6, pp. 887-896.

Gao, B.-C., M.J. Montes and C.O. Davis, 2003, "Refinement of Wavelength Calibrations of Hyperspectral Imaging Data Using a Spectrum Matching Technique," Remote Sens. Environ., in press.

Montes, M.J., B.-C. Gao and C.O. Davis, 2001, "A New Algorithm for Atmospheric Correction of Hyperspectral Remote Sensing Data," in Geo-Spatial Image and Data Exploitation II (W.E. Roper, ed.), Proceedings of the SPIE Vol. 4383, pp. 23-30.

Montes, M.J., B.-C. Gao and C.O. Davis, 2003a, "Tafkaa Atmospheric Correction of Hyperspectral Data," in Imaging Spectrometry IX (S.S. Shen and P.E. Lewis, eds.), Proceedings of the SPIE Vol. 5159, in press.

Montes, M.J., C.O. Davis, B.-C. Gao and M. Moline, 2003b, "Analysis of AVIRIS Data from LEO-15 Using Tafkaa Atmospheric Correction," 12th AVIRIS/HYPERION Earth Science Workshop (R.O. Green, ed.), Jet Propulsion Laboratory, Pasadena, California, this volume.